

CHALMERS

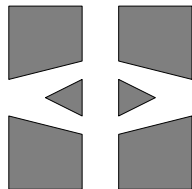
FINITE ELEMENT CENTER



PREPRINT 2002-10

Least-Squares Finite Element Methods with Applications in Electromagnetics

Rickard Bergström



Chalmers Finite Element Center

CHALMERS UNIVERSITY OF TECHNOLOGY

Göteborg Sweden 2002

CHALMERS FINITE ELEMENT CENTER

Preprint 2002-10

Least-Squares Finite Element Methods with Applications in Electromagnetics

Rickard Bergström



CHALMERS

Chalmers Finite Element Center
Chalmers University of Technology
SE-412 96 Göteborg Sweden
Göteborg, December 2002

Least-Squares Finite Element Methods with Applications in Electromagnetics

Rickard Bergström

NO 2002-10

ISSN 1404-4382

Chalmers Finite Element Center
Chalmers University of Technology
SE-412 96 Göteborg
Sweden

Telephone: +46 (0)31 772 1000

Fax: +46 (0)31 772 3595

www.phi.chalmers.se

Printed in Sweden
Chalmers University of Technology
Göteborg, Sweden 2002

Abstract

We investigate the application of the least-squares finite element method (LSFEM) to static and time harmonic Maxwell's equations in three spatial dimensions in cases of industrial significance. We find analytically and numerically that, with suitable residual weighting and mesh adaptivity, LSFEM gives satisfactory results for problems with discontinuous magnetic permeabilities of largely different orders of magnitude, but without strong corner singularities.

Least-Squares Finite Element Methods with Applications in Electromagnetics

Rickard Bergström

December 20, 2002

1 Introduction

In a least-squares finite element method (LSFEM) a sum of suitable residual norms is minimized over a piecewise polynomial space. The residuals may contain differential equations, constitutive equations, interface and boundary conditions.

LSFEM is a general method with the following features, see, e.g., Bochev and Gunzberger [5], Jiang [12], and [1]:

- applicability to general, possibly overspecified, first order systems,
- stability follows directly from well posedness of the continuous problem,
- essential boundary conditions may be imposed weakly, and
- the resulting discrete system of equations is symmetric positive definite.

In particular, LSFEM is applicable to Maxwell's equations in first order form. With the divergence equations included, LSFEM does not suffer from the spurious solutions which may occur in certain Galerkin methods, see, e.g., Jiang, Wu, and Povinelli [13] and the book by Jiang [12].

The strong norm residual minimization of LSFEM in its standard form, makes computation of singular solutions difficult. Another difficulty concerns the weighting of the different residuals. In this paper, we address these problems, with focus on static and time harmonic problems.

The paper is organized as follows. In Section 2 we present the magnetostatic problem and formulate the least-squares method, in Section 3 we prove a priori and a posteriori estimates, in Section 4 we apply the method to magnetostatic problems, and in Section 5 we extend the method to time-harmonic problems.

2 The least-squares finite element method

2.1 A magnetostatic model problem

Assume that $\Omega = \bigcup_{i=1}^n \Omega^i$ is a domain in \mathbf{R}^3 , where Ω and each Ω^i are bounded and either of class $\mathcal{C}^{1,1}$, but may be non-convex, or convex, and denote the interface between regions Ω^i and Ω^j by Γ^{ij} , with $i < j$, see Figure 1.

Let

$$\mathcal{V} = \bigoplus_{i=1}^n \mathcal{V}^i, \quad (2.1)$$

with $\mathcal{V}^i = [H^1(\Omega^i)]^3$. Assume that each subdomain have the magnetic permeability $\mu|_{\Omega^i} = \mu_r^i \mu_0$ where $\mu_r^i > 0$ is constant and μ_0 is the magnetic permeability in free space, $\mu_0 = 4\pi \times 10^{-7}$ H/m. The magnetostatic system then takes the form: find $B \in \mathcal{V}$ such that

$$\nabla \times \mu^{-1} B = J \quad \text{in } \Omega^i, \quad (2.2a)$$

$$\nabla \cdot B = 0 \quad \text{in } \Omega^i, \quad (2.2b)$$

$$B \cdot n = 0 \quad \text{on } \Gamma, \quad (2.2c)$$

and the interface conditions

$$[\mu^{-1} B \times n] = 0 \quad \text{on } \Gamma^{ij}, \quad (2.3a)$$

$$[B \cdot n] = 0 \quad \text{on } \Gamma^{ij}, \quad (2.3b)$$

hold. Here n is the exterior unit normal on the boundary Γ and a fixed unit normal on each interior interface Γ^{ij} , and $[u(x)] = \lim_{s \rightarrow 0^+} u(x + sn) - u(x - sn)$ with $x \in \Gamma^{ij}$, denotes the jump in u across the interface Γ^{ij} .

Remark 2.1 The assumption that the domains are convex or of class $\mathcal{C}^{1,1}$ is not realistic for engineering applications where we typically only have Lipschitz domains. We will discuss and relax this regularity constraint when we have proved error estimates in Section 3.

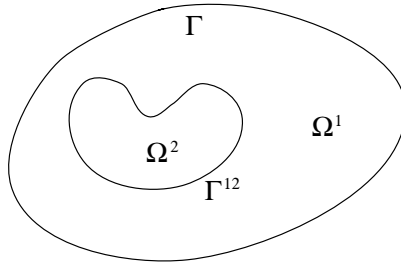


Figure 1: The notation used when a region is split into subregions.

2.2 Finite element spaces

Let $\mathcal{K}^i, i = 1, \dots, n$, be decompositions of the subdomains Ω^i into, e.g., tetrahedral, elements K , and let $\mathcal{K} = \cup_{i=1}^n \mathcal{K}^i$ denote the resulting decomposition of Ω . Let h denote the mesh function defined by $h|_K = h_K = \text{diam}(K)$, i.e., a measure of the local size of the elements in the mesh, and let $\hat{h} = \max_{K \in \mathcal{K}} h(K)$ denote the global mesh size. Non-matching meshes are allowed, but we assume local quasi-uniformity and a minimal angle condition on the triangulation, see Brenner and Scott [8]. Let

$$\mathcal{V}_h = \bigoplus_{i=1}^n \mathcal{V}_h^i, \quad (2.4)$$

with \mathcal{V}_h^i defined by

$$\mathcal{V}_h^i = \{v \in [C^0(\bar{\Omega}^i)]^3 : v|_K \in \mathcal{P}_r(K), \text{ for all } K \in \mathcal{K}^i\},$$

where \mathcal{P}_r is the set of all vector polynomials of degree less than or equal to r . Thus \mathcal{V}_h is the set of all piecewise vector polynomial functions of degree r which are continuous in the subdomains Ω^i such that, in each element, $v|_K \in \mathcal{P}_r(K)$.

For the error analysis following below, we need the following approximation property of \mathcal{V}_h , see, e.g., [14] for a proof. There is an interpolation operator $\pi = \bigoplus_{i=1}^n \pi^i$ with $\pi^i : [H^1(\Omega^i)]^3 \mapsto \mathcal{V}_h$ such that for $v \in \bigoplus_{i=1}^n [H^s(\Omega^i)]^3$, it holds

$$\|v - \pi v\|_{m,K} \leq Ch_K^{\alpha-m} |v|_{\alpha,S(K)}, \quad m = 0, 1, \quad (2.5)$$

where $\alpha = \min(r+1, s)$, $S(K)$ is the patch of elements neighboring K , and the constant C is independent of the mesh parameter h .

2.3 The least-squares finite element method with weak boundary and interface conditions

The solution B to problem (2.2)–(2.3) minimizes the least-squares functional

$$\begin{aligned} I(B) = & \sum_{i=1}^n \left(\|\mu(\nabla \times (\mu^{-1}B) - J)\|_{\Omega^i}^2 + \|\nabla \cdot B\|_{\Omega^i}^2 \right) \\ & + \sum_{1 \leq i < j \leq n} \left(\|h^{-1/2} \tilde{\mu} [\mu^{-1}B \times n]\|_{\Gamma^{ij}}^2 + \|h^{-1/2} [B \cdot n]\|_{\Gamma^{ij}}^2 \right) \\ & + \|h^{-1/2} [B \cdot n]\|_{\Gamma}^2. \end{aligned} \quad (2.6)$$

Here we have introduced a weight μ in the volume integral terms containing the curl equation. This is a natural scaling of the equations and the least-squares functional is thus better balanced between the curl and the divergence conditions. The parameter $\tilde{\mu}$ corresponds to the multiplication with μ in the volume integrals, but is an average value

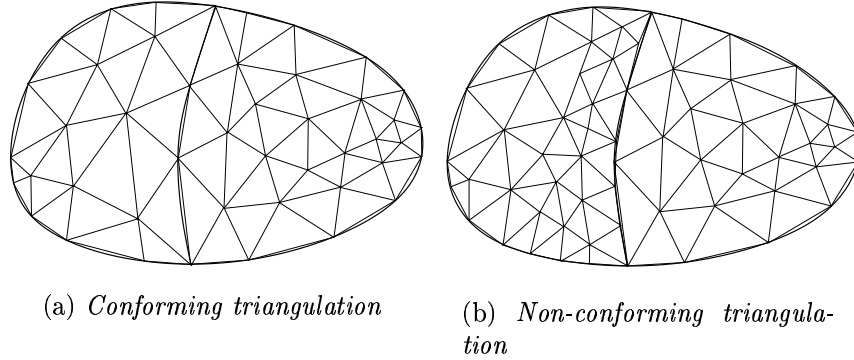


Figure 2: Examples of matching and non-matching triangulations of two subdomains. In the first case, we have the choice of both strong and weak enforcement of interface conditions. For the non-matching grid, however, we must use weak enforcement.

since μ is not defined on the interface. We will return to the exact definition of this average. Moreover, on the boundary and interfaces, the $L^2(\Gamma)$ -norm scaled by $h^{-1/2}$ has been used instead of the computationally cumbersome $H^{1/2}(\Gamma)$ -norm, see Bochev and Gunzberger [5] and the references therein. For non-matching meshes it may be necessary to use an average also for h . The least-squares method amounts to finding this minimizer: find $B \in \mathcal{V}$ such that

$$I(B) = \inf_{v \in \mathcal{V}} I(v). \quad (2.7)$$

Remark 2.2 Note that the boundary condition (2.2c) and the interface conditions (2.3) are imposed weakly. Strongly imposed boundary and interface conditions have been suggested in e.g. Jiang, Wu, and Povinelli [13], but are non-trivial to implement in polyhedral domains since the normal is not defined everywhere. Further, enforcement through the least-squares functional makes it possible to use different finite element spaces on either side of the surfaces, and the convergence properties of the method is better when using weakly imposed conditions, see Costabel and Dauge [11] and Bao and Yang [3].

A necessary condition for a function $B \in \mathcal{V}$ to satisfy equation (2.7), is

$$\lim_{\tau \rightarrow 0} \frac{\partial}{\partial \tau} I(B + \tau \tilde{B}) \equiv 2(a(B, \tilde{B}) - l(\tilde{B})) = 0, \quad (2.8)$$

for all $\tilde{B} \in \mathcal{V}$, where

$$\begin{aligned}
a(B, \tilde{B}) = & \sum_{i=1}^n (\nabla \times B, \nabla \times \tilde{B})_{\Omega^i} + (\nabla \cdot B, \nabla \cdot \tilde{B})_{\Omega^i} \\
& + \sum_{1 \leq i < j \leq n} \left((h^{-1} \tilde{\mu} [\mu^{-1} B \times n], \tilde{\mu} [\mu^{-1} \tilde{B} \times n])_{\Gamma^{ij}} \right. \\
& \quad \left. + (h^{-1} [B \cdot n], [\tilde{B} \cdot n])_{\Gamma^{ij}} \right) \\
& + (h^{-1} B \cdot n, \tilde{B} \cdot n)_{\Gamma},
\end{aligned} \tag{2.9}$$

and

$$l(\tilde{B}) = \sum_{i=1}^n (\mu J, \mu \nabla \times (\mu^{-1} \tilde{B}))_{\Omega^i}. \tag{2.10}$$

Thus seeking a minimizer to I in \mathcal{V} leads to the variational problem: find $B \in \mathcal{V}$ such that

$$a(B, \tilde{B}) = l(\tilde{B}), \tag{2.11}$$

for all $\tilde{B} \in \mathcal{V}$.

The least-squares finite element method is defined by seeking an approximation B_h in \mathcal{V}_h such that

$$I(B_h) = \inf_{v \in \mathcal{V}_h} I(v), \tag{2.12}$$

with corresponding variational form: find $B_h \in \mathcal{V}_h$ such that

$$a(B_h, \tilde{B}) = l(\tilde{B}), \tag{2.13}$$

for all $\tilde{B} \in \mathcal{V}_h$.

3 Error estimates

3.1 A priori error estimates

We begin by introducing the energy norm

$$|||v|||^2 = a(v, v) \quad \text{for } v \in \mathcal{V}, \tag{3.1}$$

Under our assumptions, $||| \cdot |||$ is a norm in \mathcal{V} when there exists a unique solution to problem (2.2)–(2.3).

Further, we have the following interpolation error estimate.

Lemma 3.1 *If $v \in \bigoplus_{i=1}^n [H^s(\Omega)]^3$, $s \geq 1$, then there is an interpolation operator $\pi : \bigoplus_{i=1}^n [H^s(\Omega)]^3 \mapsto \mathcal{V}_h$ such that*

$$|||v - \pi v||| \leq C \hat{h}^{\alpha-1} |v|_{\alpha}, \tag{3.2}$$

with $\alpha = \min(r+1, s)$ and where C only depends on μ and Ω .

Proof. Let $\eta = v - \pi v$. We show that

$$|||\eta|||^2 \leq C \sum_{K \in \mathcal{K}} h_K^{-2} \|\eta\|_K^2 + |\eta|_{1,K}^2. \quad (3.3)$$

The desired result (3.2) then follows from (2.5). For the interior terms, we directly have

$$\|\nabla \times \eta\|_K^2 \leq C |\eta|_{1,K}^2, \quad (3.4)$$

and

$$\|\nabla \cdot \eta\|_K^2 \leq C |\eta|_{1,K}^2. \quad (3.5)$$

For the boundary term we get

$$\begin{aligned} \|h^{-1/2} \eta \cdot n\|_\Gamma^2 &= \sum_{\{K \in \mathcal{K}: \partial K \cap \Gamma \neq \emptyset\}} \|h^{-1/2} \eta \cdot n\|_{\partial K \cap \Gamma}^2 \\ &\leq \sum_{\{K \in \mathcal{K}: \partial K \cap \Gamma \neq \emptyset\}} C h_K^{-1} \|\eta\|_K (h_K^{-1} \|\eta\|_K + |\eta|_{1,K}) \\ &\leq C \sum_{\{K \in \mathcal{K}: \partial K \cap \Gamma \neq \emptyset\}} h_K^{-2} \|\eta\|_K^2 + |\eta|_{1,K}^2, \end{aligned} \quad (3.6)$$

where we used the trace inequality $\|v\|_{\partial K}^2 \leq C \|v\|_K (h_K^{-1} \|v\|_K + |v|_{1,K})$. Finally, for the interface jump terms we use the triangle inequality

$$\|h^{-1/2} [\eta \cdot n]\|_{\Gamma^{ij}}^2 \leq \|h^{-1/2} \eta^i \cdot n\|_{\Gamma^i}^2 + \|h^{-1/2} \eta^j \cdot n\|_{\Gamma^j}^2, \quad (3.7)$$

and

$$\begin{aligned} \|h^{-1/2} \tilde{\mu} [\mu^{-1} \eta \times n]\|_{\Gamma^{ij}}^2 &\leq \|h^{-1/2} \tilde{\mu} (\mu^i)^{-1} \eta^i \times n\|_{\Gamma^i}^2 \\ &\quad + \|h^{-1/2} \tilde{\mu} (\mu^j)^{-1} \eta^j \times n\|_{\Gamma^j}^2, \end{aligned} \quad (3.8)$$

and then treat them with the same technique as for the boundary term. \square

Remark 3.1 If the meshes \mathcal{K}^i match on the interfaces and πv satisfies the interface conditions (2.3), then the constant C is also independent of μ since the interface terms vanish.

Now we are ready to state the following result:

Theorem 3.2 *Let $B \in \bigoplus_{i=1}^n [H^s(\Omega)]^3$ be a solution to (2.11) and $B_h \in \mathcal{V}_h$ the approximate solution defined by (2.13). Then there is a constant C , independent of h , such that*

$$|||B - B_h||| \leq C \hat{h}^{\alpha-1} |B|_\alpha, \quad (3.9)$$

with $\alpha = \min(r+1, s)$.

Proof. Let $e = B - B_h$ denote the error. Then

$$\begin{aligned} |||e|||^2 &= a(e, B - B_h) \\ &= a(e, B - \pi B + \pi B - B_h) \\ &= a(e, B - \pi B), \end{aligned} \tag{3.10}$$

where we use the Galerkin orthogonality $a(e, \tilde{B}) = 0$, for $\tilde{B} \in \mathcal{V}_h$, in the last equality. Using the Cauchy-Schwarz inequality and dividing by $|||e|||$ we arrive at

$$\begin{aligned} |||e||| &\leq |||B - \pi B||| \\ &\leq C \hat{h}^{\alpha-1} |B|_\alpha, \end{aligned} \tag{3.11}$$

where we used Lemma 3.1 in the last inequality. \square

3.2 A posteriori error estimates

A simple calculation gives that the energy norm of the error when using a bilinear form derived from least-squares principles simply equals the residual. Thus we can state the following a posteriori error estimate in the energy norm.

Theorem 3.3 *Let $B \in \mathcal{V}$ be a solution to (2.11) and $B_h \in \mathcal{V}_h$ the approximate solution defined by (2.13). Then*

$$|||B - B_h|||^2 = \sum_{K \in \mathcal{K}} \mathcal{R}_K(B_h) \cdot \mathcal{R}_K(B_h) \tag{3.12}$$

where the element residual $\mathcal{R}_K(B_h) \in \mathbf{R}^4$ is defined by

$$\mathcal{R}_K(B_h) = \begin{bmatrix} \|\mu(\nabla \times \mu^{-1} B_h - J)\|_K \\ \|\nabla \cdot B_h\|_K \\ \frac{1}{\sqrt{2}} \|h^{-1/2} \tilde{\mu}[\mu^{-1} B_h \times n]\|_{\partial K \setminus \Gamma} \\ \|\frac{1}{\sqrt{\alpha}} h^{-1/2} [B_h \cdot n]\|_{\partial K} \end{bmatrix}, \tag{3.13}$$

where α is a function, such that $\alpha = 1$ on faces F with $F \cap \Gamma \neq \emptyset$ and $\alpha = 2$ otherwise.

Remark 3.2 Under our assumptions, these results are meaningful since we have enough regularity on the solution B . In more realistic situations where Ω is only Lipschitz, we have $B \in \bigoplus_{i=1}^n [H^s(\Omega)]^3$ for $s \in (1/2, 1]$, see Amrouche, Bernardi, Dauge and Raviart [2], and the least-squares finite element method generally fails to converge to the correct solution, see e.g. Bramble, Lazarov and Pasciak [7] or the regularity results of Costabel [10]. However, the use of weak boundary and interface conditions still gives a theoretical

convergence, see Costabel and Dauge [11].

For many applications, one wants to measure the error in other quantities than the energy norm. In the remainder of this section, we use duality arguments to derive an a posteriori estimate for the error in energy,

$$W_{error} = \frac{1}{2} \int_{\Omega} \mu^{-1} |B|^2 - \frac{1}{2} \int_{\Omega} \mu^{-1} |B_h|^2. \quad (3.14)$$

Moreover, this estimate shows that we can have convergence even when $B \notin \mathcal{V}$, as is the case for a general Lipschitz domain with corners.

3.2.1 Definition of the dual problem

To prove estimates of the error in the energy, we start by studying the following problem: find $(\phi, p) \in H^s(\nabla \times, \Omega) \times H_0^1(\Omega)$ satisfying

$$\nabla \times \mu \nabla \times \phi - \nabla p = \Psi \quad \text{in } \Omega^i, \quad (3.15a)$$

$$\nabla \cdot \phi = \psi \quad \text{in } \Omega^i, \quad (3.15b)$$

$$p = 0, \quad \phi \times n = 0 \quad \text{on } \Gamma, \quad (3.15c)$$

with interface condition

$$[\mu^{-1} \phi \times n] = 0 \quad \text{on } \Gamma^{ij}, \quad (3.16a)$$

$$[\phi \cdot n] = 0 \quad \text{on } \Gamma^{ij}, \quad (3.16b)$$

$$[\mu \nabla \times \phi \times n] = 0 \quad \text{on } \Gamma^{ij}, \quad (3.16c)$$

$$[p] = 0 \quad \text{on } \Gamma^{ij}. \quad (3.16d)$$

Here we introduced the space $H^s(\nabla \times, \Omega) = \{v \in [H^s(\Omega)]^3 : \nabla \times v \in [H^s(\Omega)]^3\}$. This problem is analysed in Chen, Du, and Zou [9], where it is shown that there exists a unique solution. Furthermore, $p \equiv 0$ for all Ψ with $\nabla \cdot \Psi = 0$.

3.2.2 Estimate of the error in energy

Using the Helmholtz decomposition, see e.g. Bossavit [6], we can write the error $e = B - B_h = B^0 - (B_h^0 + B_h^\perp)$, where we have $\nabla \cdot F^0 = 0$, and $F^\perp = \nabla f$ for some scalar function f . We choose

$$\Psi = B^0 + B_h^0, \quad (3.17)$$

making $\nabla \cdot \Psi = 0$ and thus $p = 0$, and ψ such that it satisfies the auxiliary weak problem: find $\psi \in H^1(\Omega)$ such that

$$(\nabla \psi, \nabla v) = \sum_{i=1}^n (\nabla \cdot (\mu^{-1} B_h^\perp), v)_{\Omega^i} - \sum_{1 \leq i < j \leq n} ([\mu^{-1} B_h^\perp \cdot n], v)_{\Gamma^{ij}}, \quad (3.18)$$

for all $v \in H^1(\Omega)$. This problem is well posed and we have the equality $-(\nabla\psi, B_h^\perp) = (\mu^{-1}B_h^\perp, B_h^\perp)$ since B_h^\perp is a gradient of a scalar function.

Taking the inner product of (3.15a) with $\mu^{-1}e^0 = \mu^{-1}(B^0 - B_h^0)$ and of (3.15b) with $\nabla \cdot e^\perp = -\nabla \cdot B^\perp$, yields for the right hand side

$$\begin{aligned}
& (\mu^{-1}B^0, B^0) - (\mu^{-1}B_h^0, B_h^0) - (\psi, \nabla \cdot B_h^\perp) \\
&= (\mu^{-1}B^0, B^0) - (\mu^{-1}B_h^0, B_h^0) + (\nabla\psi, B_h^\perp) \\
&\quad - (\psi, [B_h^\perp \cdot n])_\Gamma - \sum_{1 \leq i < j \leq n} (\psi, [B_h^\perp \cdot n])_{\Gamma^{ij}} \\
&= W_{error} - (\nabla \cdot \phi, [B_h^\perp \cdot n])_\Gamma - \sum_{1 \leq i < j \leq n} (\nabla \cdot \phi, [B_h^\perp \cdot n])_{\Gamma^{ij}}.
\end{aligned} \tag{3.19}$$

We thus get

$$\begin{aligned}
W_{error} &= \sum_{i=1}^n \left((\mu^{-1}B^0, B^0)_{\Omega^i} - (\mu^{-1}B_h^0, B_h^0)_{\Omega^i} - (\mu^{-1}B_h^\perp, B_h^\perp)_{\Omega^i} \right) \\
&\quad + \sum_{1 \leq i < j \leq n} (\nabla \cdot \phi, [B_h^\perp \cdot n])_{\Gamma^{ij}} + (\nabla \cdot \phi, [B_h^\perp \cdot n])_\Gamma \\
&= \sum_{i=1}^n \left((\nabla \times \mu \nabla \times \phi, \mu^{-1}e^0)_{\Omega^i} - (\nabla p, \mu^{-1}e^0)_{\Omega^i} + (\nabla \cdot \phi, \nabla \cdot e^\perp)_{\Omega^i} \right) \\
&\quad + \sum_{1 \leq i < j \leq n} (\nabla \cdot \phi, [e^\perp \cdot n])_{\Gamma^{ij}} + (\nabla \cdot \phi, [e^\perp \cdot n])_\Gamma \\
&= \sum_{i=1}^n \left((\nabla \times \phi, \nabla \times e^0)_{\Omega^i} + (\nabla \cdot \phi, \nabla \cdot e^\perp)_{\Omega^i} + (\mu^{-1}p, \nabla \cdot e^0)_{\Omega^i} \right) \\
&\quad + \sum_{1 \leq i < j \leq n} \left((\mu \nabla \times \phi, [\mu^{-1}e^0 \times n])_{\Gamma^{ij}} + (\mu^{-1}p, [e^\perp \cdot n])_{\Gamma^{ij}} + (\nabla \cdot \phi, [e^\perp \cdot n])_{\Gamma^{ij}} \right) \\
&\quad + (\nabla \cdot \phi, [n \cdot e^\perp])_\Gamma \\
&= \sum_{i=1}^n \left((\nabla \times \phi, \nabla \times e)_{\Omega^i} + (\nabla \cdot \phi, \nabla \cdot e)_{\Omega^i} \right) \\
&\quad + \sum_{1 \leq i < j \leq n} \left((\mu \nabla \times \phi, [\mu^{-1}e \times n])_{\Gamma^{ij}} + (\nabla \times \phi, [e \cdot n])_{\Gamma^{ij}} \right) + (\nabla \times \phi, [e^\perp \cdot n])_\Gamma \\
&= \sum_{i=1}^n \left((\nabla \times (\phi - \pi\phi), \nabla \times e)_{\Omega^i} + (\nabla \cdot (\phi - \pi\phi), \nabla \cdot e)_{\Omega^i} \right) \\
&\quad + \sum_{1 \leq i < j \leq n} \left((h^{1/2}\tilde{\mu}^{-1}\mu \nabla \times \phi + h^{-1/2}[\mu^{-1}(\phi - \pi\phi) \times n], \tilde{\mu}h^{-1/2}[\mu^{-1}e \times n])_{\Gamma^{ij}} \right. \\
&\quad \quad \left. + (h^{1/2}\nabla \cdot \phi + h^{-1/2}[(\phi - \pi\phi) \cdot n], h^{-1/2}[e \cdot n])_{\Gamma^{ij}} \right) \\
&\quad + (h^{1/2}\nabla \cdot \phi + h^{-1/2}[(\phi - \pi\phi) \cdot n], h^{-1/2}[e \cdot n])_\Gamma.
\end{aligned} \tag{3.20}$$

The following estimate for the error in the energy is thereby proved.

Theorem 3.4 *Let ϕ be the solution to (3.15) with data according to (3.17) and (3.18), B the solution of (2.11), and B_h the LSFEM approximation (2.13), then the error in energy is bounded as*

$$W(B) - W(B_h) \leq \sum_{K \in \mathcal{K}} \mathcal{R}_K(B_h) \cdot \mathcal{W}_K(\phi), \quad (3.21)$$

where the elementwise residual $\mathcal{R}_K(B_h)$ is defined in (3.13) and the element weight $\mathcal{W}_K(\phi)$ is

$$\mathcal{W}_K(\phi) = \begin{bmatrix} \|\nabla \times (\phi - \pi\phi)\|_K \\ \|\nabla \cdot (\phi - \pi\phi)\|_K \\ \frac{1}{\sqrt{2}} \|h^{1/2} \tilde{\mu}^{-1} \mu \nabla \times \phi + h^{-1/2} [\mu^{-1} (\phi - \pi\phi) \times n]\|_{\partial K \setminus \Gamma} \\ \|\frac{1}{\sqrt{\alpha}} h^{1/2} \nabla \cdot \phi + h^{-1/2} [(\phi - \pi\phi) \cdot n]\|_{\partial K} \end{bmatrix}, \quad (3.22)$$

with α as in (3.13).

Remark 3.3 Assuming $\phi \in \bigoplus_{i=1}^n [H^{s_\phi}(\Omega)]^3$ and $B \in \bigoplus_{i=1}^n [H^{s_B}(\Omega)]^3$, the most important consequence of Theorem 3.4 is that for a geometry such that $s_\phi + s_B > 2$, we have convergence in the energy even if convergence in the solution itself can not be proved. The analysis in [9] and [2] makes it reasonable to believe that $s_\phi \geq 2s_B$, with $s_B \in (1/2, 1]$, making this true in many cases. A fact further indicated by our numerical experiments.

4 Two magnetostatic problems

4.1 Computational set up

Although not explicitly mentioned in the previous sections, one may also weight the different terms in the least-squares functional by constants without changing the analysis. We have used this possibility to make the enforcement of the interface terms stronger. For the first problem we weighted the terms containing the normal components by a factor 10^3 , while the tangential condition was left unweighted. For the second problem considered, we weighted the tangential condition by a factor 10^3 and left the normal condition unweighted. This choice of coefficients has been based on numerical experiments.

Adaptivity was based on the a posteriori result in Theorem 3.4, and an assumed regularity $s_\phi = 4/3$ of ϕ , the solution to the dual problem. We have thus not solved the dual problem numerically. The element indicator used was then

$$I_K = h_K^{1/3} \mathcal{R}_K(B_h), \quad (4.1)$$

with $\mathcal{R}_K(B_h)$ as in equation (3.13).

	Linear	Quadratic	Reference
No of elements	505 710	247 800	-
No of nodes	91 510	339 936	-
W_{air} (J)	$8.967 \times 10^{-7}(0.013)$	$9.081 \times 10^{-7}(0.001)$	9.089×10^{-7}
W_{cu} (J)	$3.333 \times 10^{-8}(0.078)$	$3.581 \times 10^{-8}(0.009)$	3.614×10^{-8}
W_{fe} (J)	$4.885 \times 10^{-10}(0.033)$	$4.802 \times 10^{-10}(0.015)$	4.731×10^{-10}

Table 1: The computed magnetic energies for Problem 1, using LSFEM and piecewise linear and quadratic polynomial elements, compared with reference values; the relative error is given in parenthesis. The reference values are from two dimensional computations done at ABB [4].

4.2 Problem 1

4.2.1 Description of the problem

The geometry of this problem is described in Figure 4(a). The problem is axisymmetric in order to make two dimensional computations possible as reference. A three dimensional view can be seen in Figure 5. The model consists of an iron cylinder core encircled by a copper winding. The configuration is enclosed in air and surrounded by a box with perfectly conducting surfaces. The winding is modelled as a homogeneous copper coil.

Data for this problem are relative magnetic permeabilities $\mu_{r,Fe} = 10^4$ and $\mu_{r,Cu} = \mu_{r,air} = 1$ and $\mu_0 = 4\pi \times 10^{-7}$ H/m and the current density J is constant over the cross section of the coil and the total current is 1 A.

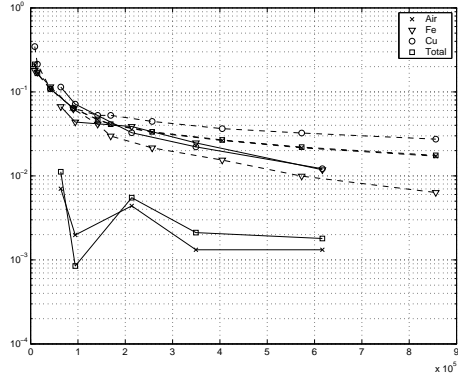
Reference computations in two dimensions done by ABB and reported in [4], gave the values of the magnetic energies in the different materials as listed in Table 1, where the magnetic energy is defined by

$$W_{\Omega^i} = \frac{1}{2} \int_{\Omega^i} B \cdot H \, dx. \quad (4.2)$$

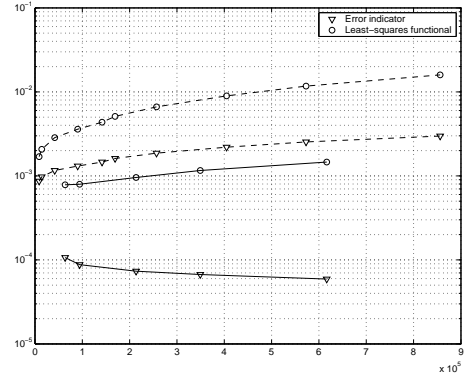
4.2.2 Computational results

This problem was solved successfully to good accuracy, see Table 1. A field line plot is shown in Figure 5. In Figure 3(a) we plot the relative error in the magnetic energy as a function of the degrees of freedom, N , for quadratic and linear polynomial basis functions, and in Figure 3(b) the error indicator (4.1) and the least-squares functional are plotted.

We can note that the rate of convergence is the same for both linear and quadratic polynomials due to the low regularity of the problem, only the accuracy is different. Another indicator of the low regularity is that the least-squares functional does not decrease with refinement, in fact it increases. However, the increase is smaller with quadratic polynomials.

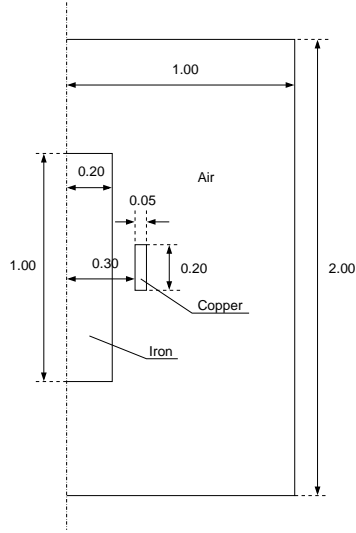


(a) *Relative error in energy in the different parts*

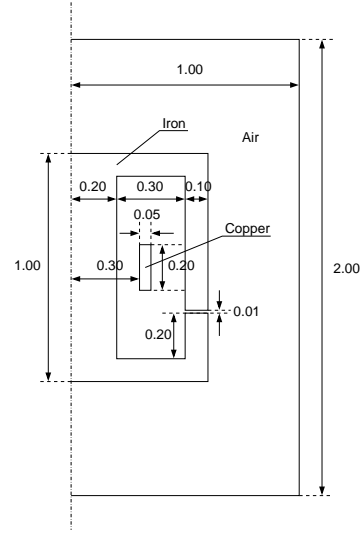


(b) *Error indicator and least-squares functional*

Figure 3: Computations for Problem 1 with quadratic (solid lines) and linear (dashed lines) basis functions.



(a) *Problem 1*



(b) *Problem 2*

Figure 4: Geometry of the two axisymmetric problems. The dimensions are given in meters.

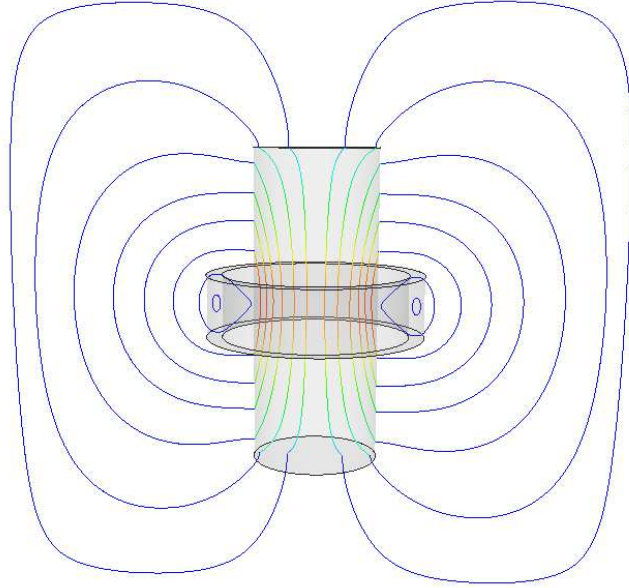


Figure 5: The magnetic field lines in a slice through the three dimensional solution of the axisymmetric Problem 1.

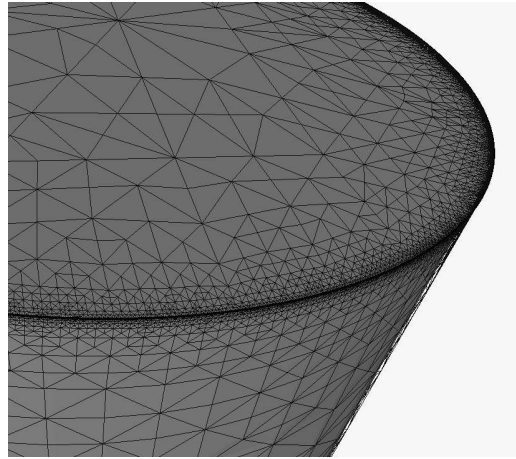


Figure 6: Detail of the mesh after adaptive refinement. The part shown is the top of the iron core of Problem 1.

	Linear	Quadratic	Reference
No of elements	1267028	198863	-
No of nodes	258537	261362	-
W_{air} (J)	$8.199 \times 10^{-7}(0.200)$	$7.573 \times 10^{-7}(0.261)$	1.025×10^{-6}
W_{cu} (J)	$3.274 \times 10^{-8}(0.086)$	$3.345 \times 10^{-8}(0.066)$	3.596×10^{-8}
W_{fe} (J)	$2.113 \times 10^{-6}(0.407)$	$1.516 \times 10^{-6}(0.575)$	3.564×10^{-6}

Table 2: The computed magnetic energies for Problem 2, using LSFEM and piecewise linear and quadratic polynomial elements, compared with reference values. The reference values are from two dimensional computations done at ABB [4].

4.3 Problem 2

4.3.1 Description of the problem

The second problem is also an axisymmetric magnetostatic problem, but the geometry is more complicated than in Problem 1. It is given in Figure 4(b). The copper winding is the same, but the iron part has been extended and almost encloses the coil. The problem has been tested with $\mu_{r,Fe} = 10^4$ as well as with $\mu_{r,Fe} = 10^2$, the other data are the same as in Problem 1.

4.3.2 Results

This problem has not been satisfactorily solved with LSFEM. For the case with $\mu_{r,Fe} = 10^2$ we still have convergence, but with poor accuracy, see Figure 7 and Table 2. The computations with $\mu_{r,Fe} = 10^4$ is not successful and not reported further.

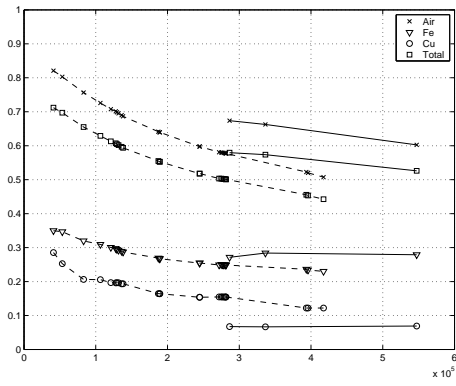
We can also see that the use of quadratic polynomials does not give better results, the singularities are too dominant in this geometry.

5 Extension to the time-harmonic case

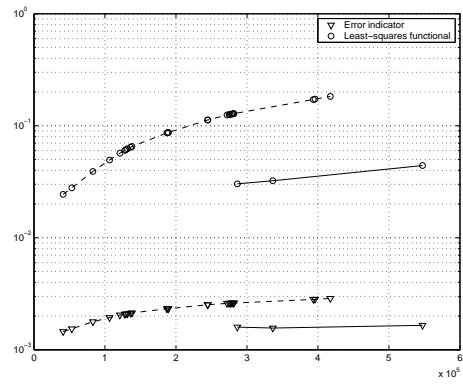
5.1 Description of the problem

As a third problem the “asymmetrical conductor with a hole problem” [15], as illustrated in Figure 10, has been used. It consists of an aluminium plate with a hole, placed under a copper winding, modeled as a homogeneous coil. There are no symmetries in this problem. The aluminium plate has a conductivity of $\sigma = 3.526 \times 10^7$ S/m and the magnetic permeability is $\mu_{r,Al} = 1$, as in the air and the copper. Since no magnetic material is present there are no singularities as in the previous two problems. Instead, we will get induced eddy currents in the conducting aluminium plate.

The coil is carrying a sinusoidal total current of 2742 A. The frequency is 50 Hz and the current density is constant over the cross section.



(a) *Relative error in energy in the different parts*



(b) *Error indicator and least-squares functional*

Figure 7: Computations for Problem 2 with quadratic (solid lines) and linear (dashed lines) basis functions.

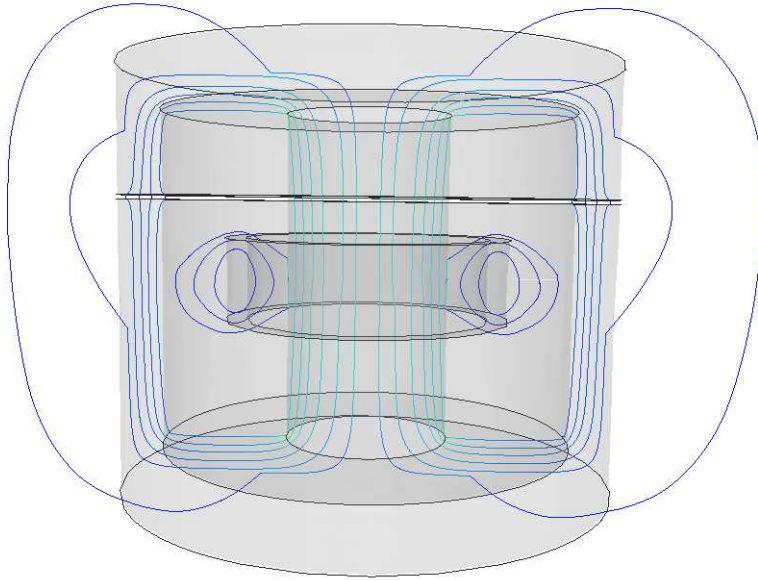


Figure 8: The magnetic field lines in a slice through the three dimensional solution of the axisymmetric Problem 2.

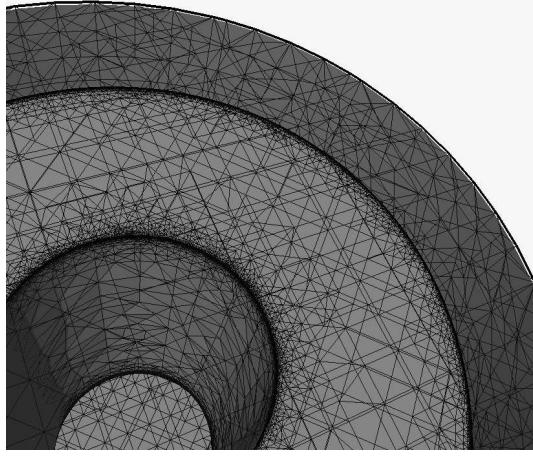


Figure 9: Detail of the mesh after adaptive refinement. The part shown is a top view of the interior of the iron core of Problem 2.

5.2 The equations

Since the current is sinusoidal and the frequency is low, we use the quasistatic time-harmonic equations

$$\nabla \times E = -j\omega B \quad \text{in } \Omega^i, \quad (5.1a)$$

$$\nabla \times H = J \quad \text{in } \Omega^i, \quad (5.1b)$$

$$\nabla \cdot B = 0 \quad \text{in } \Omega^i, \quad (5.1c)$$

where

$$B = \mu H, \quad (5.2a)$$

$$J = J_{sc} + \sigma E. \quad (5.2b)$$

Note that equation (5.1b) implies that $\nabla \cdot J = 0$. The interface conditions for this problem then becomes

$$[E \times n] = 0 \quad \text{on } \Gamma^{ij}, \quad (5.3a)$$

$$[H \times n] = 0 \quad \text{on } \Gamma^{ij}, \quad (5.3b)$$

$$[J \cdot n] = 0 \quad \text{on } \Gamma^{ij}, \quad (5.3c)$$

$$[B \cdot n] = 0 \quad \text{on } \Gamma^{ij}, \quad (5.3d)$$

where n is a unit normal to the interface and $[\cdot]$ denotes the jump across the surface as before. Since $\mu_r = 1$ in the whole region, the magnetic field is continuous over surfaces. The same is true for the tangential component of the electric field, E_t , while (5.3c) implies that $E_{Al}^+ \cdot n = 0$, where E_{Al}^+ denotes the field inside the aluminium plate, since $J = 0$ in the air. No further restrictions apply on the electric field.

The boundary conditions applied are

$$E \times n = 0 \quad \text{on } \Gamma, \quad (5.4a)$$

$$B \cdot n = 0 \quad \text{on } \Gamma. \quad (5.4b)$$

The placement of the outer boundary is not specified in description of the test case. We have enclosed the coil and the aluminium plate in a cube of approximately three times the size of a side in the plate.

5.3 The least-squares formulation

Even though the magnetic field is continuous in the whole region, we still have to introduce the discontinuous elements along the surfaces, due to the jump in the normal component of E . Setting up the least-squares functional for this system of equations then leads to the following expression,

$$\begin{aligned} I(E, H) = & \sum_{i=1}^3 \left(\|\nabla \times E + j\omega\mu H\|_{\Omega^i}^2 \right. \\ & \left. + \|\nabla \times H - \sigma E - J_{sc}\|_{\Omega^i}^2 + \|\nabla \cdot (\mu H)\|_{\Omega^i}^2 \right) \\ & + \sum_{1 \leq i < j \leq 3} \left(\|h^{-1/2} [E \times n]\|_{\Gamma_{ij}}^2 + \|h^{-1/2} E^+ \cdot n\|_{\Gamma_{Al}}^2 \right) \\ & + \sum_{1 \leq i < j \leq 3} \left(\|h^{-1/2} [H \times n]\|_{\Gamma_{ij}}^2 + \|h^{-1/2} [\mu H \cdot n]\|_{\Gamma_{ij}}^2 \right) \\ & + \|h^{-1/2} [E \times n]\|_{\Gamma}^2 + \|h^{-1/2} [\mu H \cdot n]\|_{\Gamma}^2, \end{aligned} \quad (5.5)$$

where the second of the interface terms signify that the normal component of the E field inside the aluminium should be zero on the interface.

The conditions for a minimum of $I(E, H)$ give the following variational formulation for $U = (E, H)$: find U such that

$$a_{\Omega}(U, \tilde{U}) + a_1(U, \tilde{U}) + a_2(U, \tilde{U}) + a_3(U, \tilde{U}) = l(\tilde{U}), \quad (5.6)$$

for all \tilde{U} , where

$$\begin{aligned} a_{\Omega}(U, \tilde{U}) = & \sum_{i=1}^3 (\nabla \times E + j\omega\mu H, \nabla \times \tilde{E} + j\omega\mu \tilde{H})_{\Omega^i} \\ & + (\nabla \times H - \sigma E, \nabla \times \tilde{H} - \sigma \tilde{E})_{\Omega^i} \\ & + (\nabla \cdot (\mu H), \nabla \cdot (\mu \tilde{H}))_{\Omega^i}, \end{aligned} \quad (5.7a)$$

$$l(\tilde{U}) = \sum_{i=1}^3 (J_{sc}, \nabla \times \tilde{H} - \sigma \tilde{E})_{\Omega^i}. \quad (5.7b)$$

and for the interface terms,

$$a_1(U, \tilde{U}) = \sum_{1 \leq i < j \leq 3} (h^{-1}[E \times n], [\tilde{E} \times n])_{\Gamma^{ij}} \quad (5.8a)$$

$$a_2(U, \tilde{U}) = \sum_{1 \leq i < j \leq 3} \left((h^{-1}[H \times n], [\tilde{H} \times n])_{\Gamma^{ij}} + (h^{-1}E^+ \cdot n, \tilde{E}^+ \cdot n)_{\Gamma_{Al}}, \right. \\ \left. + (h^{-1}[\mu H \cdot n], [\mu \tilde{H} \cdot n])_{\Gamma^{ij}} \right), \quad (5.8b)$$

$$a_3(U, \tilde{U}) = (h^{-1}[E \times n], [\tilde{E} \times n])_{\Gamma} + (h^{-1}[\mu H \cdot n], [\mu \tilde{H} \cdot n])_{\Gamma}. \quad (5.8c)$$

Note that in these expressions we are dealing with complex vector fields. In practise, one separates the real and imaginary parts and thus has to work with 12 unknown variables.

5.4 Computational results

As expected, in the absence of singularities, this problem could be solved successfully with LSFEM. Comparison with experimental data is shown in Figure 11(a). The currents induced in the aluminium plate are shown in Figure 12. However, due to the size of the problem, we have only been able to compute using linear polynomial basis functions and not reaching the desired accuracy. The convergence though is good as shown in Figure 11(b), since the L^2 norm of the residual is equivalent to the error in energy norm.

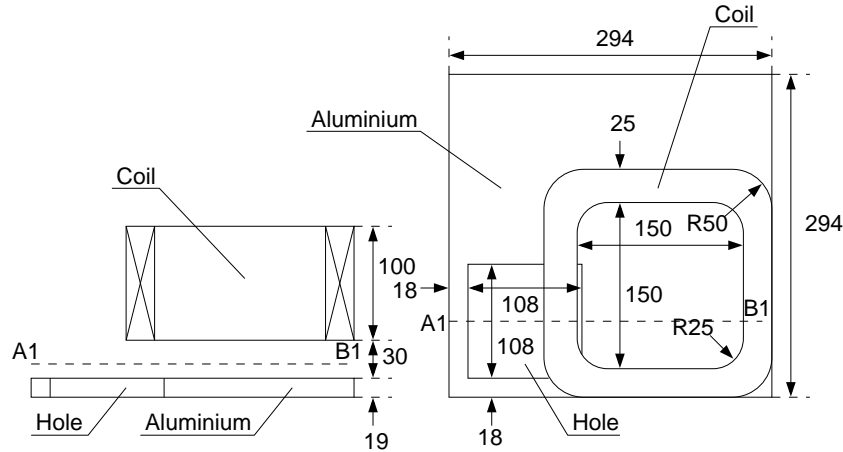
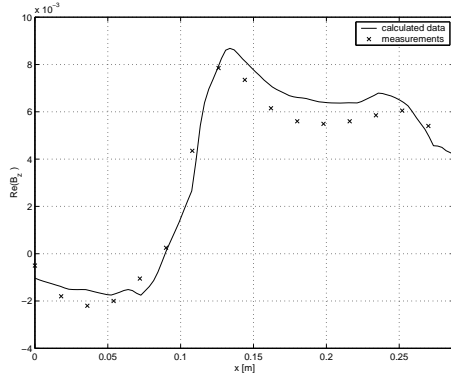
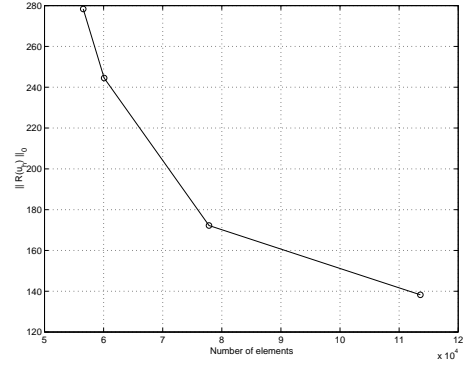


Figure 10: The geometry of Problem 3, a) front view, b) top view. The dimensions are given in millimeters.

In this example we do not have an increasing residual, see Figure 11(b), which caused problems in the previous examples. Hence, it has been possible to use the least-squares



(a) Comparison with experimental data taken along line A1-B1 in Figure 10.



(b) The least-squares functional during refinement

Figure 11: Computations for Problem 3 with linear basis functions.

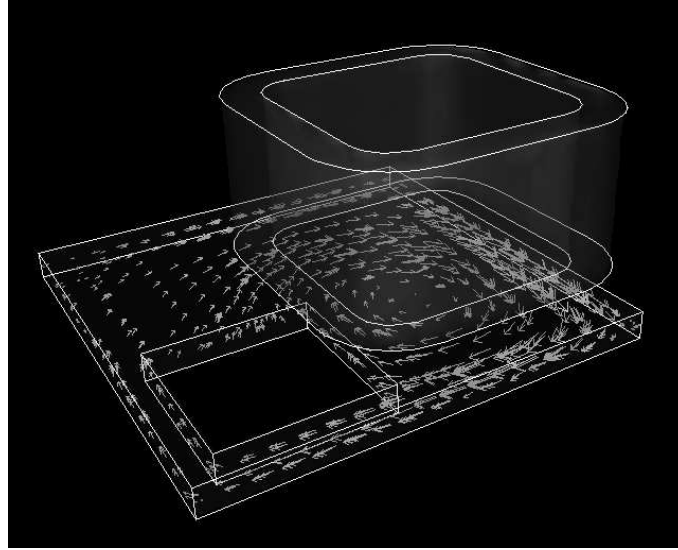


Figure 12: Vector plot of the induced current in the aluminium plate of Problem 3.

residual as refinement criterion:

$$\begin{aligned} I_K = & \|\nabla \times E + j\omega\mu H\|_K^2 \\ & + \|\nabla \times H - \sigma E - J_{sc}\|_K^2 \\ & + \|\nabla \cdot (\mu H)\|_K^2, \end{aligned} \tag{5.9}$$

References

- [1] First-order system least squares philosophy.
`ftp://amath.colorado.edu/pub/fosls/FOSLoSophy.ps`.
- [2] C. Amrouche, C. Bernardi, M. Dauge, and V. Girault. Vector potentials in three-dimensional nonsmooth domains. *Math. Methods Appl. Sci.*, 21:823–864, 1998.
- [3] G. Bao and H. Yang. A least-squares finite element analysis for diffraction problems. *SIAM J. Numer. Anal.*, 37(2):665–682, 2000.
- [4] R. Bergström, A. Bondeson, C. Johnson, M.G. Larson, Y. Liu, and K. Samuelsson. Adaptive finite element methods in electromagnetics. Technical Report 2, Swedish Institute of Applied Mathematics (ITM), 1999.
- [5] P.B. Bochev and M.D. Gunzburger. Finite element methods of least-squares type. *SIAM Rev.*, 40(4):789–837, 1998.
- [6] A. Bossavit. *Computational Electromagnetism*. Academic Press, 1998.
- [7] J.H. Bramble, R.D. Lazarov, and J.E. Pasciak. A least-squares approach based on a discrete minus one inner product for first order systems. *Math. Comp.*, 66(219):935–955, 1997.
- [8] S.C. Brenner and L.R. Scott. *The Mathematical Theory of Finite Element Methods*. Springer-Verlag, 1994.
- [9] Z.M. Chen, Q. Du, and J. Zou. Finite element methods with matching and nonmatching meshes for Maxwell equations with discontinuous coefficients. *SIAM J. Numer. Anal.*, 37:1542–1570, 2000.
- [10] M. Costabel. A coercive bilinear form for Maxwell’s equations. *J. Math. Anal. Appl.*, 157(2):527–541, 1991.
- [11] M. Costabel and M. Dauge. Un résultat de densité pour les équations de Maxwell régularisées dans un domaine lipschitzien. *C. R. Acad. Sci. Paris Sér. I Math.*, 327(9):849–854, 1998.
- [12] B.-N. Jiang. *Least-squares finite element method : Theory and applications in computational fluid dynamics and electromagnetics*. Springer-Verlag, 1998.
- [13] B.-N. Jiang, J. Wu, and L.A. Povinelli. The origin of spurious solutions in computational electromagnetics. *J. Comp. Phys.*, 125:104–123, 1996.
- [14] L.R. Scott and S. Zhang. Finite element interpolation of nonsmooth functions satisfying boundary conditions. *Math. Comp.*, 54:483–493, 1990.

- [15] L. Turner. Benchmark problems for the validation of eddy current computer codes. *COMPEL*, 9:123–216, 1990.

Chalmers Finite Element Center Preprints

- 2001–01** *A simple nonconforming bilinear element for the elasticity problem*
Peter Hansbo and Mats G. Larson
- 2001–02** *The \mathcal{LL}^* finite element method and multigrid for the magnetostatic problem*
Rickard Bergström, Mats G. Larson, and Klas Samuelsson
- 2001–03** *The Fokker-Planck operator as an asymptotic limit in anisotropic media*
Mohammad Asadzadeh
- 2001–04** *A posteriori error estimation of functionals in elliptic problems: experiments*
Mats G. Larson and A. Jonas Niklasson
- 2001–05** *A note on energy conservation for Hamiltonian systems using continuous time finite elements*
Peter Hansbo
- 2001–06** *Stationary level set method for modelling sharp interfaces in groundwater flow*
Nahidh Sharif and Nils-Erik Wiberg
- 2001–07** *Integration methods for the calculation of the magnetostatic field due to coils*
Marzia Fontana
- 2001–08** *Adaptive finite element computation of 3D magnetostatic problems in potential formulation*
Marzia Fontana
- 2001–09** *Multi-adaptive galerkin methods for ODEs I: theory & algorithms*
Anders Logg
- 2001–10** *Multi-adaptive galerkin methods for ODEs II: applications*
Anders Logg
- 2001–11** *Energy norm a posteriori error estimation for discontinuous Galerkin methods*
Roland Becker, Peter Hansbo, and Mats G. Larson
- 2001–12** *Analysis of a family of discontinuous Galerkin methods for elliptic problems: the one dimensional case*
Mats G. Larson and A. Jonas Niklasson
- 2001–13** *Analysis of a nonsymmetric discontinuous Galerkin method for elliptic problems: stability and energy error estimates*
Mats G. Larson and A. Jonas Niklasson
- 2001–14** *A hybrid method for the wave equation*
Larisa Beilina, Klas Samuelsson and Krister Åhlander
- 2001–15** *A finite element method for domain decomposition with non-matching grids*
Roland Becker, Peter Hansbo and Rolf Stenberg
- 2001–16** *Application of stable FEM-FDTD hybrid to scattering problems*
Thomas Rylander and Anders Bondeson
- 2001–17** *Eddy current computations using adaptive grids and edge elements*
Y. Q. Liu, A. Bondeson, R. Bergström, C. Johnson, M. G. Larson, and K. Samuelsson

- 2001–18** *Adaptive finite element methods for incompressible fluid flow*
Johan Hoffman and Claes Johnson
- 2001–19** *Dynamic subgrid modeling for time dependent convection–diffusion–reaction equations with fractal solutions*
Johan Hoffman
- 2001–20** *Topics in adaptive computational methods for differential equations*
Claes Johnson, Johan Hoffman and Anders Logg
- 2001–21** *An unfitted finite element method for elliptic interface problems*
Anita Hansbo and Peter Hansbo
- 2001–22** *A P^2 –continuous, P^1 –discontinuous finite element method for the Mindlin-Reissner plate model*
Peter Hansbo and Mats G. Larson
- 2002–01** *Approximation of time derivatives for parabolic equations in Banach space: constant time steps*
Yubin Yan
- 2002–02** *Approximation of time derivatives for parabolic equations in Banach space: variable time steps*
Yubin Yan
- 2002–03** *Stability of explicit-implicit hybrid time-stepping schemes for Maxwell’s equations*
Thomas Rylander and Anders Bondeson
- 2002–04** *A computational study of transition to turbulence in shear flow*
Johan Hoffman and Claes Johnson
- 2002–05** *Adaptive hybrid FEM/FDM methods for inverse scattering problems*
Larisa Beilina
- 2002–06** *DOLFIN - Dynamic Object oriented Library for FINite element computation*
Johan Hoffman and Anders Logg
- 2002–07** *Explicit time-stepping for stiff ODEs*
Kenneth Eriksson, Claes Johnson and Anders Logg
- 2002–08** *Adaptive finite element methods for turbulent flow*
Johan Hoffman
- 2002–09** *Adaptive multiscale computational modeling of complex incompressible fluid flow*
Johan Hoffman and Claes Johnson
- 2002–10** *Least-squares finite element method with applications in electromagnetics*
Rickard Bergström

These preprints can be obtained from

www.phi.chalmers.se/preprints